Key role of the N-terminus of chicken annexin A5 in vesicle aggregation

Javier Turnay, Ana Guzmán-Aránguez, Emilio Lecona, Juan I. Barrasa, Nieves Olmo, and M[a] Antonia Lizarbe*

Departamento de Bioquímica y Biología Molecular I, Facultad de Ciencias Químicas, Universidad Complutense, 28040-Madrid, Spain

Received 3 November 2008; Accepted 27 February 2009
DOI: 10.1002/pro.119
Published online 16 March 2009 proteinscience.org

Abstract: Annexins are calcium-dependent phospholipid-binding proteins involved in calcium signaling and intracellular membrane trafficking among other functions. Vesicle aggregation is a crucial event to make possible the membrane remodeling but this process is energetically unfavorable, and phospholipid membranes do not aggregate and fuse spontaneously. This issue can be circumvented by the presence of different agents such as divalent cations and/or proteins, among them some annexins. Although human annexin A5 lacks the ability to aggregate vesicles, here we demonstrate that its highly similar chicken ortholog induces aggregation of vesicles containing acidic phospholipids even at low protein and/or calcium concentration by establishment of protein dimers. Our experiments show that the ability to aggregate vesicles mainly resides in the N-terminus as truncation of the N-terminus of chicken annexin A5 significantly decreases this process and replacement of the N-terminus of human annexin A5 by that of chicken switches on aggregation; in both cases, there are no changes in the overall protein structure and only minor changes in phospholipid binding. Electrostatic repulsions between negatively charged residues in the concave face of the molecule, mainly in the N-terminus, seem to be responsible for the impairment of dimer formation in human annexin A5. Taking into account that chicken annexin A5 presents a high sequence and structural similarity with mammalian annexins absent in birds, as annexins A3 and A4, some of the physiological functions exerted by these proteins may be carried out by chicken annexin A5, even those that could require calcium-dependent membrane aggregation.

Keywords: calcium binding; circular dichroism spectroscopy; crosslinking; fluorescence emission spectroscopy; liposomes; phospholipid binding

Introduction

Annexins constitute a superfamily of calcium-dependent membrane-binding proteins that are mainly intracellular and are involved in a wide variety of intra- and extracellular functions.[1–3] The ability to interact with acidic phospholipids lies in a highly conserved protein core composed of four homologous domains (eight in annexin A6); each conserved domain within the protein core is folded into five α helices and these, in turn, are wound into a right-handed super-helix. The four domains are packed into a disc-shaped structure with a slightly convex face where the type-2 calcium and phospholipid binding loops are located. The concave face, which is opposite to the membrane-binding surface, is mainly formed by the "C" helices of

Abbreviations: bA4, bovine annexin A4; cA5, chicken annexin A5; cNt-hA5, chimera of human annexin A5 protein core with the N-terminus from chicken annexin A5; dnt-cA5, chicken annexin A5 with deleted N-terminus; hA5, human annexin A5; HTS, heparin tetrasaccharide [$\Delta^{4,5}$-2-O-sulfo-uronic acid(1→4)-2-deoxy-2-sulfamido-α-D-glucopyranosyl-6-O-sulfate(1→4)-2-O-sulfo-α-L-iduronic acid(1→4)-2-deoxy-2-sulfamido-α-D-glucopyranosyl-6-O-sulfate]; IPTG, isopropyl-β-D-thiogalactopyranoside; PC, phosphatidylcholine; PG, phosphatidylglycerol; PS, phosphatidylserine.

Grant sponsor: The Ministerio de Ciencia e Innovación (Spain); Grant numbers: BFU2005-02671 and BFU2008-04758.

*Correspondence to: M[a] Antonia Lizarbe, Dpto. Bioquímica y Biología Molecular I, Facultad de Ciencias Químicas, Universidad Complutense, 28040—Madrid, Spain.
E-mail: lizarbe@bbm1.ucm.es

each domain together with the N-terminal extension that closes the structure by bringing together domains I and IV. The N-terminal domain shows the greatest variability within annexins both in length and amino acid composition, ranging from a few residues, as in annexin A5, to 200 or more residues (i.e., annexin A11). Although this extension is markedly smaller than the protein core, it greatly influences the overall protein stability and determines the structural arrangement of protein regions located in the opposite side of the molecule.[4] In addition, specific functions of each annexin and their regulation are mainly dependent on this variable extension.[4,5]

Annexins are involved in several physiological functions, among them membrane trafficking, endo and exocytosis, and in the interaction between membranes and the cytoskeleton; for several of these functions, annexins not only require their binding to membranes but they must also show an ability to act as protein bridges between membranes. Several vertebrate annexins, including annexins A1, A2, A4, and A7, are able to aggregate phospholipid-containing vesicles when bound to membranes,[6–10] whereas others as annexins A3, A5, A6, A11, and nonmyristoylated A13b do not promote aggregation.[6,11,12] This process is negatively regulated by phosphorylation of the N-terminal domain at serine/threonine and tyrosine residues[5,13] or by proteolysis of the N-terminal extension.[14]

A prerequisite for aggregation is that annexins must bind first to the vesicles. In a second step, it has been described that aggregation is induced by two different potential mechanisms. The first model assumes that vesicle aggregation results from the interaction of annexin molecules bound to different vesicles via protein–protein interaction (dimer formation or establishment of heterotetramers with proteins from the S100 family).[7,14–16] The second model proposes that annexins may reveal a secondary phospholipid binding site in their N-terminus after binding to a vesicle through the primary binding site, thus establishing a single annexin protein bridge.[9,10,14,17]

Human annexin A5 (hA5) has been used as a model of nonmembrane aggregating annexin and used to construct chimeras to verify that the vesicle aggregation ability of annexin A1 (one of the most extensively studied aggregation-inducing annexins) lies in its N-terminal domain.[14,18,19] However, during the purification and characterization of chicken annexin A5 (cA5) and its truncated mutant lacking eight amino acids from the N-terminus (dnt-cA5), we found some experimental evidences that suggested that this annexin, in contrast to its mammal orthologs, did induce vesicle aggregation.[20–22] In view of the relevance that vesicle aggregation has for membrane trafficking, we decided to confirm the anomalous behavior of cA5 and to further investigate the structural determinant of the vesicle aggregation activity of cA5. As the N-terminus of annexins is their major regulatory domain, we have centred this study mainly in this region; thus, we have studied the effect of a partial truncation of the N-terminus and constructed a chimera comprising the N-terminus of cA5 and the protein core of hA5 (cNt-hA5). In addition, we discuss whether cA5 may assume functions exerted in mammalians by annexins with a high degree of sequence similarity with cA5 but whose genes are absent in birds (e.g., annexins A4 and to a lower extent A3).

Results

Cloning, purification and structural characterization of the recombinant proteins

We have previously obtained and characterized cA5 and a mutant with a deletion of eight amino acids from the N-terminus (dnt-cA5), as well as hA5.[20–22] Here, we have cloned a chimera comprising the N-terminus of cA5 and the protein core of hA5 [(Fig. 1(A,B)]. This chimera, as well as recombinant cA5, hA5, and dnt-cA5, were purified from JA221 *E. Coli* cultures transformed with the corresponding constructs after induction with 1 m*M* IPTG. The final protein preparations obtained after DEAE-cellulose chromatography were free of any detectable contaminations after analysis by SDS-PAGE followed by silver nitrate staining. Figure 1(C) shows the electrophoretic analysis of the material from different steps in the purification of cNt-hA5 after Coomassie blue staining or Western blot using anti-hA5 antibodies. The reversible interaction of cNt-hA5 with phosphatidylserine (PS) vesicles indicates that the chimera is functional regarding its ability to bind to acidic phospholipids. Moreover, CD spectroscopy reveals the correct folding of the proteins and that the secondary structure of cNt-hA5 is almost identical to hA5 (see Fig. 2). On the other hand, cA5 and its truncated form show slightly higher negative ellipticity values mainly at the 222 nm minimum. In any case, analysis of the spectra using the algorithm described by Perczel et al.[23] does not reveal significant variations in the overall α-helical content and only minor variations in the β-sheet and random coil percentages (cA5 and dnt-cA5: 80–81% α-helix, 0–1% β-sheet, 5% β-turns, and 14% random coil; hA5 and cNt-hA5: 77–78% α-helix, 0% β-sheet, 11% β-turns, and 11–12% random coil). More significant changes are observed when thermal unfolding is considered (Fig. 2, Inset). The most stable protein is cA5 with a melting temperature (T_m) of 59.2 ± 0.4°C; truncation of the N-terminus is accompanied by a highly significant decrease in T_m (around 7°C). hA5 and the chimeric protein cNt-hA5 show a quite similar thermal unfolding (T_m, 50.2°C) that surprisingly is even lower than that of truncated dnt-cA5. The final heat-unfolded state seems to differ from chicken to human annexins, although in all of the cases the process is irreversible; hA5 and cNt-hA5 show an apparent intermediate state at around 60°C with high

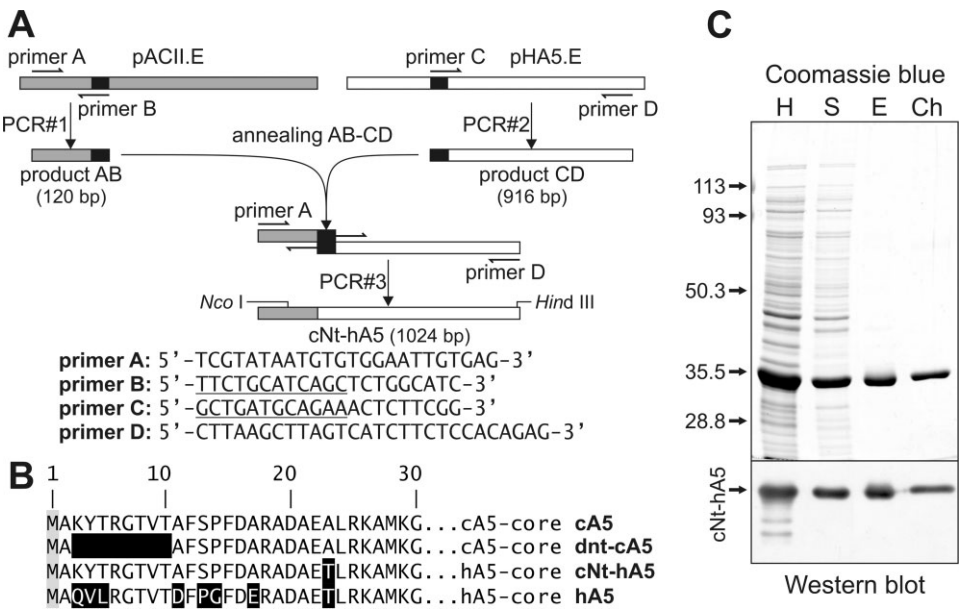

Figure 1. Construction and expression of the cNt-hA5 chimera. (**A**) Scheme of the splicing by overlap extension technique used for the construction of cNt-hA5; primers sequences are indicated. (**B**) Sequences of the N-terminal domains are given in the one letter code; reverse shading indicates residues that differ between cA5 and hA5. (**C**) Purification steps during cNt-hA5 purification followed by SDS-PAGE and Coomassie blue staining (upper panel) and Western blot using polyclonal antibodies against hA5. Exponentially growing pcNt-cA5.E transformed JA221 *E. coli* cultures were induced for 16 h with 1 m*M* IPTG, centrifuged and homogenized by sonication in the presence 2.5 m*M* EGTA (H); after centrifugation for 1 h at 35,000*g* and 4°C, the supernatant (S) was decanted and PS-enriched liposomes (1 mg/mL) and $CaCl_2$ (2 m*M* final concentration) were added. Interaction with liposomes was allowed for 30 min at 4°C and the vesicles were sedimented by centrifugation, washed with buffer containing 1 m*M* $CaCl_2$ and finally, the recombinant protein was extracted from the vesicles by resuspension in buffer containing 5 m*M* EGTA and centrifugation (E). A final ion-exchange chromatographic purification step in DEAE-cellulose yielded the cNt-hA5 preparation (Ch).

β-sheet content (>50%), whereas cA5 and dnt-cA5 do not. This is probably due to a faster macroscopical aggregation of denatured chicken annexins, whereas this process is slower in the human counterparts.

Interaction with acidic phospholipid vesicles

Binding of the recombinant annexins to PS liposomes was studied by ultracentrifugation using 400 nm vesicles (600:1 lipid:protein molar ratio) and increasing $CaCl_2$ concentration (see Fig. 3). Calcium dependence for binding was quite similar between chicken and human intact proteins (around 45–50 μ*M* $CaCl_2$ for 50% binding) with slightly higher calcium requirements for truncated dnt-cA5 and for the chimera (around 70 μ*M*). In all of the cases, the behavior was highly cooperative and annexins were completely bound at 100–150 μ*M* $CaCl_2$ under these experimental conditions.

In addition, binding was analyzed by fluorescence emission spectroscopy using unilamellar 50 nm PS-vesicles. Figure 4 shows the spectra obtained for the four recombinant proteins in the absence of calcium and PS (dashed lines) and in the presence of 200 μ*M* $CaCl_2$ and increasing PS to protein molar ratios. cA5 and dnt-cA5 spectra are unaffected by addition of 200 μ*M* Ca^{2+}, but hA5 spectrum shows a 7-nm shift in its maximum; cNt-hA5 shows an intermediate

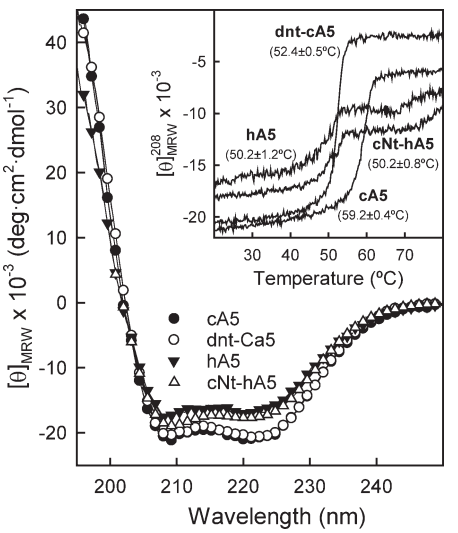

Figure 2. Far-UV circular dichroism spectra and thermal stability of purified recombinant proteins. Spectra were registered at 20°C in 20 m*M* Hepes, pH 7.4, containing 0.1*M* NaCl, and using protein preparations around 0.3 mg/mL. Inset: Thermal unfolding curves determined by monitorization of ellipticity changes at 208 nm between 20 and 80°C and increasing temperature at 60°C/h. Melting temperatures (T_m) are shown and correspond to mean values (±SD) of at least three independent determinations.

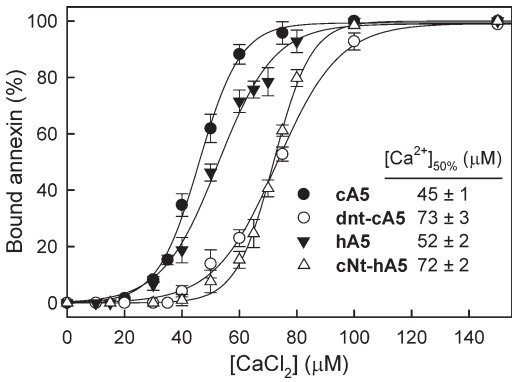

Figure 3. Liposome sedimentation assay comparing calcium dependence of the binding of recombinant proteins to PS unilamellar vesicles. Binding of recombinant proteins to 400 nm unilamellar PS vesicles was analyzed by ultracentrifugation in the presence of calcium concentrations ranging from 0 (1 m*M* EGTA) to 200 μ*M*. Pellets were analyzed by SDS-PAGE followed by Coomassie blue staining and densitometry. Data represent means (±SD) of at least three independent experiments.

behavior showing only a 2-nm shift in the spectrum. A more significant shift in the maximum towards higher wavelengths, together with an increase in the quantum yield (higher in cA5 and dnt-cA5 when compared with proteins with the human core), was observed in the four recombinant proteins when PS-vesicles are added in the presence of 200 μ*M* Ca^{2+}. This confirms that the conformational rearrangement that exposes Trp^{187} after binding to phospholipid vesicles takes place not only in the intact proteins but also in dnt-cA5 and cNt-hA5.

Fluorescence emission spectra were analyzed and the ratio between fluorescence intensities at wavelengths corresponding to the emission maxima of completely bound or free annexin was plotted vs. the PS to protein molar ratio (see Fig. 5). This analysis reveals that half-maximal binding to 50-nm PS vesicles in the presence of 200 μ*M* Ca^{2+} is achieved at PS to protein molar ratios ranging from 20 (cA5) to 45 (cNt-hA5). A more profound analysis of the binding data (Fig. 5 insets) reveals that the number of phospholipid molecules in the bilayers involved in binding of one molecule of annexin is quite similar for all the recombinant proteins (around 20) and that apparent dissociation constants are in the low micromolar range, being lowest for cA5 (1.2 μ*M*) and highest for the chimera (5.3 μ*M*).

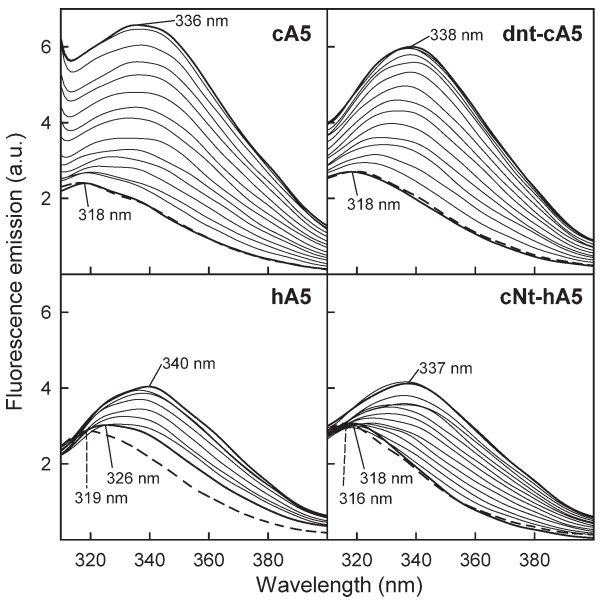

Figure 4. Fluorescence emission spectra of recombinant annexins bound to PS unilamellar vesicles. The influence of the lipid to protein molar ratio in the binding of the recombinant proteins to 50 nm PS unilamellar vesicles was analyzed by fluorescence emission spectroscopy. Spectra of the unique Trp residue present in the four recombinant proteins in the absence of calcium and PS (dashed lines) or in the presence of 200 μ*M* $CaCl_2$ at increasing lipid to protein molar ratio (thicker lines represent [L]/[P] = 0 and 120) are shown. The wavelengths corresponding to the maxima of the most significant spectra are shown.

Induction of vesicle aggregation

Once we had verified that all the recombinant proteins were able to bind to acidic phospholipid bilayers, we analyzed the ability to induce vesicle aggregation under different conditions (see Fig. 6). We have found that hA5 does not induce aggregation even at high

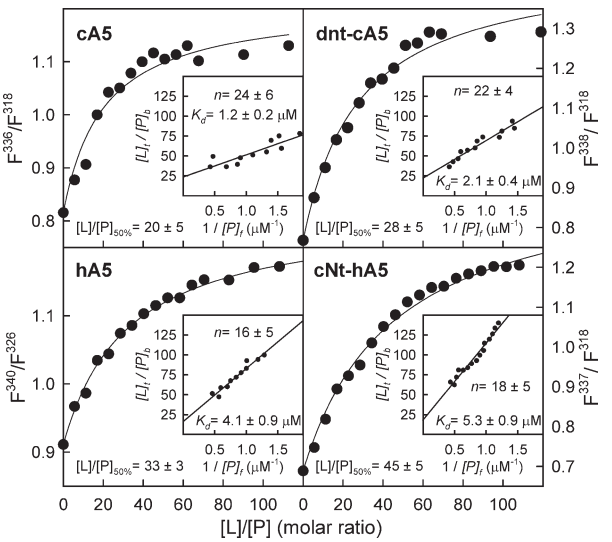

Figure 5. Analysis of the fluorescence emission spectra of recombinant annexins bound to PS unilamellar vesicles. Spectra from Figure 4 were analyzed and the main plots show the ratio between fluorescence intensities at wavelengths corresponding to the emission maxima of completely bound or free annexin in the presence of 200 μ*M* $CaCl_2$. The ratio required for 50% binding ($[L]/[P]_{50\%}$) under these experimental conditions is indicated. Insets: plots of $[L]_t/[P]_b$ vs. $1/[P]_f$ for each recombinant protein showing the values obtained for apparent K_d and *n*.

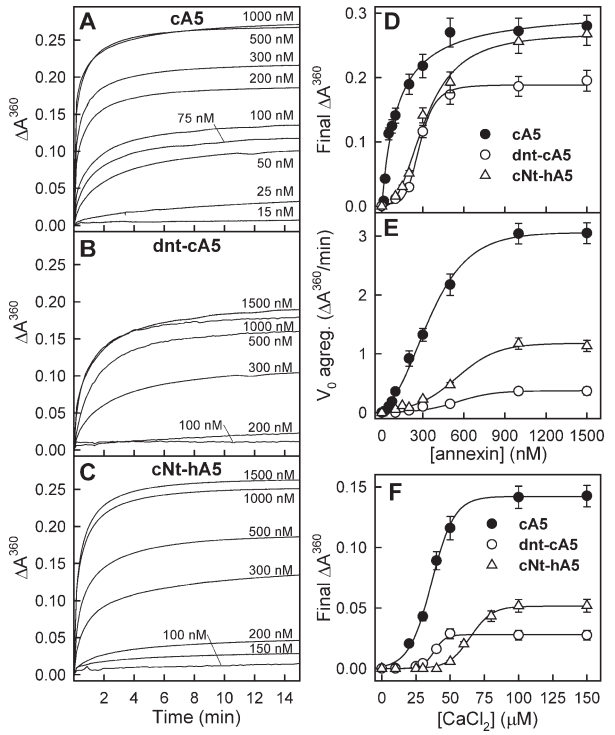

Figure 6. Annexin-induced vesicle aggregation. (**A–C**) Aggregation of 100 nm unilamellar PS vesicles was studied as a function of protein concentration in the presence of 200 μ*M* $CaCl_2$. Aggregation was initiated by adding Ca^{2+} to a suspension of vesicles at the indicated protein concentration in 20 m*M* Hepes, pH 7.4, 0.1*M* NaCl, and was followed by continuously monitoring absorbance at 360 nm in a thermostatized cuvette at 20°C. hA5 did not induce aggregation even at high protein concentration (2 μ*M*) and $CaCl_2$ up to 1 m*M*. (**D, E**) Aggregation curves in A–C were analyzed to determine the values of final ΔA^{360} and apparent initial aggregation velocity (V_0). The former parameter was determined from the non-linear regression to a hyperbola of the aggregation curve up to 15 min, whereas apparent V_0 was determined from the analysis of the data up to only 1 min. (**F**) Calcium dependence of annexin-induced vesicle aggregation was carried out as previously described but maintaining constant protein concentration (100 n*M* for cA5 and 200 n*M* for dnt-cA5 and cNt-hA5) and inducing aggregation by adding Ca^{2+} to achieve different final concentrations (up to 200 μ*M*). Maximum ΔA^{360} was determined as described above. Data in D–F correspond to mean values (±SD) of three different experiments.

protein or calcium concentrations in accordance with previous reports[6]; on the other hand, cA5 induces this process even at very low protein concentration [above 15 n*M*; Fig. 6(A)]. Moreover, calcium requirements for aggregation are even lower than those required for maximal binding under identical lipid:protein molar ratio [$[Ca^{2+}]_{50\%} = 36 \pm 1$ μ*M*; Fig. 6(F) when compared with Fig. 3], indicating that the aggregation process can be triggered by the binding of a small number of annexin molecules to the vesicles. The relevance of the N-terminal extension of chicken annexin A5 for the induction of vesicle aggregation is put forward by the fact that truncation of this extension significantly decreases the vesicle aggregation ability of cA5. Figure 6(B) shows that, under identical experimental conditions, dnt-cA5 requires 10 times higher protein concentration than cA5 to be able to detect vesicle aggregation. The analysis of maximal ΔA^{360} and apparent initial velocity of aggregation [Fig. 6(D,E)] also clearly show that the removal of eight amino acids from the N-terminus impairs aggregation induced by the chicken annexin. More interestingly, the cNt-hA5 chimera, where the N-terminus of hA5 is replaced by that of cA5, gains the ability to induce vesicle aggregation [Fig. 6(C)] although to a lower extent than cA5 [lower final ΔA^{360} values at low protein concentration and lower apparent initial velocity; Fig. 6(D,E)]. Calcium requirements for aggregation are higher than those required by cA5 or dnt-cA5 in good agreement with the higher requirements also detected for binding to phospholipid vesicles.

The physiological relevance of the vesicle aggregation ability of cA5 was confirmed at the normal body temperature of the chicken (around 42°C). Figure 7(A) shows the PS aggregation curves at 42°C; time scale is expanded as the aggregation process showed higher apparent initial velocity rates at this temperature when compared with 20°C [Fig. 7(B)]. Calcium dependence for aggregation shows a more cooperative behavior at 42°C [Fig. 7(C)] than at 20°C [Fig. 6(F)] and a higher value of $[Ca^{2+}]_{50\%}$ (94 ± 2 μ*M*); in any case, maximal induction of aggregation is induced *in vitro* at similar concentrations (over 100 μ*M* Ca^{2+}). Although it is not physiologically relevant, dnt-cA5 and cNt-hA5 also induced vesicle aggregation at 42°C and, as expected, hA5 did not either at 37 or at 42°C (data not shown).

The analysis of the initial aggregation rates is dependent on cA5 concentration at 20 and 42°C [Figs. 6(E) and 7(B)]. Double logarithmic plots of the values obtained at high lipid to protein molar ratios (over 1000-fold, where free lipid concentration can be considered constant), yield linear representations with slopes close to 2 [1.86 and 1.82 at 20 and 42°C, respectively; Fig. 7(B) inset]. Therefore, the aggregation process produced by cA5 is second order in protein concentration under these conditions indicating that the aggregation of PS vesicles by cA5 proceeds via formation of a protein dimer at the initial step.

Crosslinking of vesicle associated annexins

An experimental approach to detect protein to protein interactions was designed by inducing lysine crosslinking using BS^3 under conditions of low and high occupancy of the outer layers of the vesicle membranes varying the lipid:protein molar ratio (600:1 and 100:1, respectively) (see Fig. 8). First, we verified that no intermolecular crosslinking was detected in the four recombinant proteins in solution (No PS) or in the presence of PS vesicles but in the absence of calcium

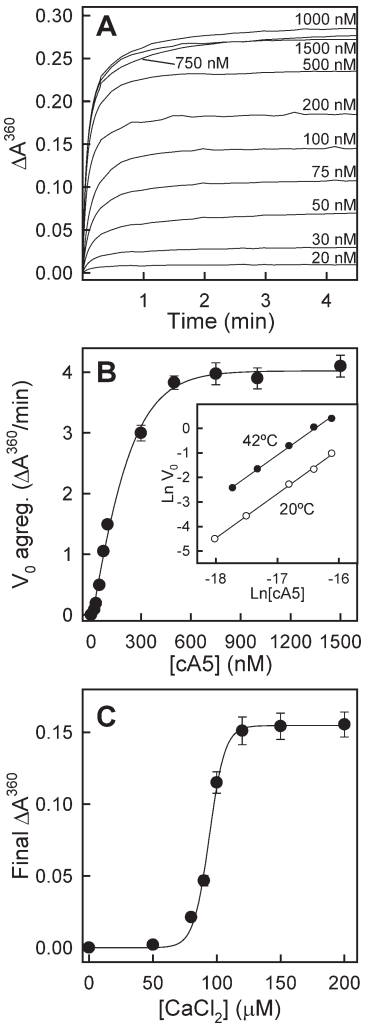

Figure 7. cA5-induced vesicle aggregation at chicken physiological temperature. Experiments were carried out as in Figure 6 but in a thermostatized cuvette at 42°C. (**A**) Aggregation curves at different cA5 concentrations. (**B**) Analysis of the apparent initial aggregation rates; the Inset shows the double logarithmic plot of initial aggregation rates vs. cA5 concentration at lipid to protein molar ratios larger than 1000 (below 100 n*M* cA5). (**C**) Calcium dependence of cA5-induced vesicle aggregation was carried out maintaining constant protein concentration (100 n*M*) and inducing aggregation by adding Ca^{2+} to achieve different final concentrations (up to 200 μ*M*). Data in B and C correspond to mean values (±SD) of three different experiments.

(1 m*M* EGTA). In some cases, mainly in hA5 and cNt-hA5, intramolecular crosslinking occurred and a double monomer band could be observed as a consequence of an improper unfolding by SDS.[24,25] When crosslinking was carried out at a 100:1 lipid:protein molar ratio, lateral interactions among annexin molecules bound to the same vesicle are detected. Dimers, trimers, and higher molecular weight oligomers can be observed in the four proteins bound to PS vesicles, as it is shown for cA5 and hA5 in Figure 8. This observation is in good agreement with the well described ability of annexin A5 from different origins to oligomerize and form 2D crystals of trimers on the bilayer surface[26–30] through an interfacial basic cluster in which at least one lysine residue is involved (Lys[29]) and several other are at crosslinking distance.[28]

When the crosslinking experiments are carried out at low membrane occupancy (600:1 lipid:protein molar ratio; 0.5 μ*M* protein; 200 μ*M* $CaCl_2$), under conditions equivalent to the aggregation assays, hA5 does not induce vesicle aggregation and interestingly, no oligomerization is observed (see Fig. 8). On the contrary, cA5 shows a strong band corresponding to a protein dimer and almost no higher molecular weight oligomers are observed (see Fig. 8). Dimer formation is also observed in the other two recombinant proteins that induce vesicle aggregation, the N-terminally truncated mutant dnt-cA5 and in the chimera cNt-hA5.

Inhibition of vesicle aggregation by heparin tetrasaccharide

Heparin tetrasaccharide [HTS; ΔUA,2S(1→4)-α-D-GlcNS,6S(1→4)-α-L-IdoUA,2S(1→4)-α-D-GlcNS,6S] has been reported to bind with high affinity to rat annexin A5[31] at two basic amino acid clusters located in the concave face of the molecule, and with lower affinity to an additional site in the convex side. These sites are highly conserved in cA5; thus, we assayed the influence of binding of HTS to cA5 in vesicle aggregation, as HTS would bind to the exposed concave faces of the vesicle bound annexin molecules. As binding of HTS requires high calcium concentrations (around

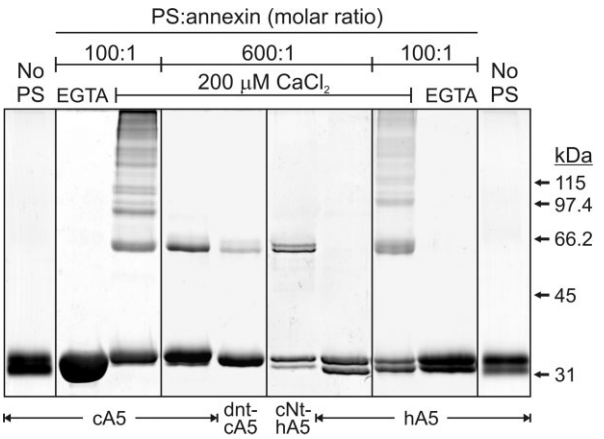

Figure 8. Crosslinking of annexins bound to PS unilamellar vesicles. Crosslinking of recombinant annexins was carried out at 100:1 and 600:1 phospholipid to annexin molar ratio in the presence of 200 μ*M* Ca^{2+} using BS^3; after stopping the crosslinking reaction, samples were centrifuged and the vesicle-bound annexin was analyzed. Controls were carried out in the presence of PS but without calcium (1 m*M* EGTA) or in the presence of calcium but without liposomes; in these cases, almost no annexin was sedimented and crosslinking was evaluated in aliquots from the supernatnats ("EGTA" and "No PS").

5 m*M*), we changed the phospholipid liposome composition from PS to an equimolecular mixture of phosphatidylglycerol and phosphatidylcholine (PG:PC) as these liposomes do not self-aggregate at 5 m*M* calcium [Fig. 9(B)]. Binding of cA5 (100 n*M*) to 100 nm PG:PC vesicles (~130 μ*M*) in the presence of 5 m*M* $CaCl_2$ was complete and not affected by the presence of a 500-fold molar excess of HTS [Fig. 9(A)]. On the other hand, preincubation of cA5 with HTS in the presence of 5 m*M* $CaCl_2$ induced an HTS concentration-dependent inhibition of aggregation with around a 50% decrease in the initial aggregation rates and final ΔA^{360} values [Fig. 9(B,C)].

Discussion

Human annexin A5 has been reported as one of the members of this family of proteins that does not induce vesicle aggregation. However, we have previously described the cloning and structural-functional characterization of its chicken counterpart and our experimental data suggested that cA5 does induce this process.[20–22] The N-terminus of these proteins is considered as their major regulatory domain and several relevant differences are found in this extension between cA5 and hA5. Therefore, we decided to analyze whether the N-terminus of annexin A5 was responsible for the on/off switch of the vesicle aggregating activity. For this purpose, we purified recombinant cA5 and hA5 as well as a truncated mutant of the former that lacks residues 3–10 located in the N-terminus (dnt-cA5). In addition, we have cloned, expressed, and purified a chimera with the N-terminus of cA5 and the protein core of hA5. The comparative analysis of the secondary structure of the four recombinant proteins reveals that they are correctly folded and that the secondary structure and the thermal stability of the chimera are quite similar to those of hA5. Although the alteration of the N-terminus of annexin A5 does not significantly affect its secondary structure, some slight differences can be found in the binding capacity of the mutated annexins to PS vesicles. Calcium dependence for PS-binding is lower for the non-mutated proteins (45–50 μ*M* Ca^{2+} for half-maximal binding), being around 20 μ*M* higher for truncated dnt-cA5 and for the chimera cNt-hA5. Thus, alterations in the N-terminus are translated into subtle structural changes that affect the calcium and phospholipid binding sites located in the protein core on the opposite side of the molecule, as we have previously reported.[5,21,22] Calcium concentrations over

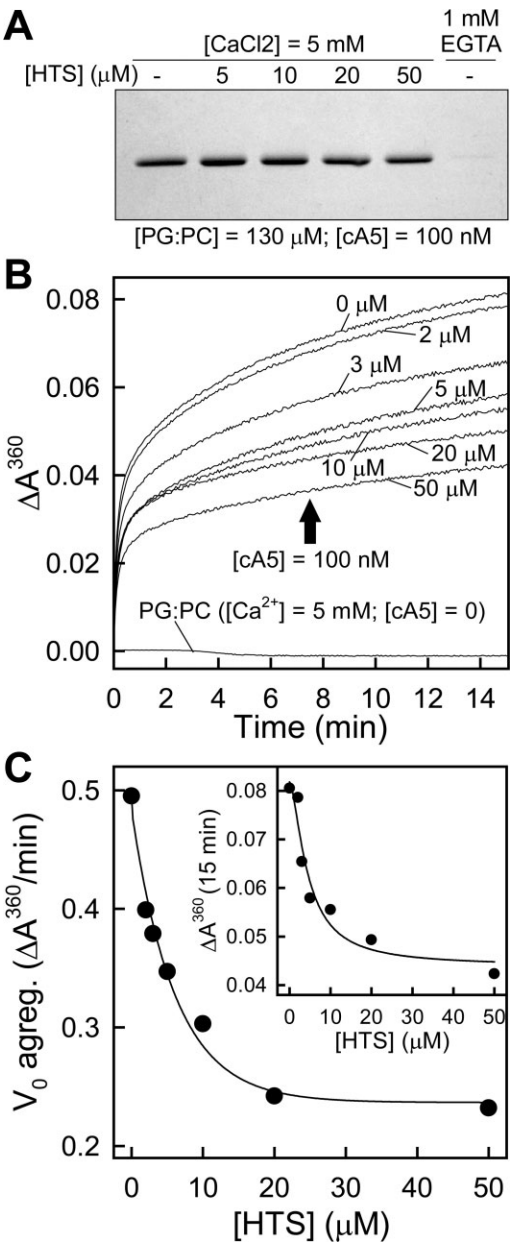

Figure 9. Inhibition of cA5-induced vesicle aggregation by heparin tetrasaccharide. The effect of HTS binding in cA5-induced vesicle aggregation was assayed after preincubation of cA5 with increasing concentrations of HTS in the presence of 5 m*M* $CaCl_2$ at 20°C. Afterwards, aggregation was triggered by addition of a concentrated stock of unilamellar 100 nm PG:PC liposomes. (**A**) Influence of HTS in the binding of cA5 to PG:PC vesicles was analyzed under identical experimental conditions to those used for the aggregation studies. 100 nm cA5-containing unilamellar vesicles were centrifuged in a Beckman Coulter Optima MAX-XP ultracentrifuge at 150,000*g* for 1 h at 4°C and the sediment and supernatants were analyzed by SDS-PAGE followed by Coomassie blue staining and densitometric analysis of the protein bands. A negative control without calcium (1 m*M* EGTA) was included. Total cA5 sedimentation was achieved in the absence of HTS and only a minor reduction in sedimentation (<7%) was observed at the highest HTS concentration used. (**B**) cA5-induced aggregation curves at increasing HTS concentration; no aggregation of PG:PC vesicles at 5 m*M* $CaCl_2$ was observed in the absence of cA5 either in the absence or presence of HTS. (**C**) Analysis of the apparent initial aggregation velocity and ΔA^{360} after 15 min as a function of HTS concentration.

100 μM induce total binding of the four proteins to PS-vesicles; these are the conditions used throughout the experiments herein reported.

The fluorescence emission spectra of Trp^{187} in the absence of calcium and phospholipids correspond, in the four proteins, to a completely buried residue with emission maxima ranging from 316 to 319 nm. Addition of 200 μM $CaCl_2$ only affects hA5 spectrum with a red shift in the tryptophan emission maximum of 7 nm and an increase in the quantum yield. This effect is due to calcium-induced structural rearrangements in the protein core after calcium binding that increase the exposure of Trp^{187}. Lower calcium affinity of chicken annexins is likely responsible for the absence of this effect in cA5 and dnt-cA5.[21] The cNt-hA5 chimera does not present such a significant shift as the intact hA5, what confirms the influence of the N-terminal extension on the protein core. Calcium affinity is strongly increased when ternary complexes with phospholipids are formed[15] and this is reflected in immediate changes in the fluorescence spectra of all recombinant proteins. After addition of PS-vesicles, the Trp^{187} emission maxima shift towards 340 nm and an increase in the quantum yield is observed, as has been already described for hA5.[32] The increase in the quantum yield is due to the loss of the strong quenching of Trp^{187} through hydrogen bonding to Thr^{224} that takes place in the calcium-free conformation. Upon calcium binding, mild acidification or interaction with acidic phospholipids, the loop connecting helices A and B in domain III changes its conformation exposing Trp^{187} to the solvent or to the polar heads of the phospholipids breaking the interaction with Thr^{224}.[22,33]

cA5 binds to PS-vesicles in the presence of 200 μM Ca^{2+} with an apparent higher affinity than hA5, reflected in a lower value of the lipid to protein molar ratio for half maximal binding (20 for cA5 vs. 33 for hA5) and in a lower apparent dissociation constant (1.2 μM for cA5 vs. 4.1 μM for hA5). As in the sedimentation assays, fluorescence spectra confirm that alteration of the N-terminal domain modifies the affinity of the resulting annexin molecule for PS-vesicles. dnt-cA5 and the chimera show a higher apparent dissociation constant than cA5 and hA5, respectively. However, these changes do not modify the number of phospholipid molecules required in both leaflets for binding to the liposomes (around 20 in the four proteins).

Once we verified the correct folding of the recombinant proteins and their calcium-dependent binding to PS-vesicles, we checked their potential ability to induce vesicle aggregation. The data demonstrate that chicken annexin A5, in contrast to its human ortholog, is able to induce this process even at low protein and calcium concentrations, either at 20°C or at the normal body temperature of the chicken (around 42°C). Moreover, the results obtained with the N-terminally truncated mutant and the chimera with the N-terminus of cA5 reveal that the short N-terminal extension of cA5 is essential for the induction of vesicle aggregation. However, additional regions of the protein core must be involved in this process, as truncation of the N-terminus does not completely abolish aggregation and replacement of the N-terminus of hA5 by that of cA5 does not yield a protein with the same aggregation ability as cA5.

As the apparent initial velocity values do not decrease at high protein concentration [Fig. 6(E)], the aggregation is probably triggered by the interaction between two proteins bound to different vesicles rather than by a single protein bridge. The kinetic analysis of the initial aggregation rates at high lipid to protein molar ratio indicates that this process is second order in protein concentration, which strongly supports this hypothesis. These data, together with cross-linking experiments show that cA5-induced membrane aggregation is most likely mediated by the dimerization of cA5 molcules on different vesicles. Taking into account that HTS binding to the concave exposed surface of annexin A5 strongly impairs vesicle aggregation, it could be suggested that dimerization takes place via these surfaces. HTS does not completely impair aggregation as it is not covalently bound to cA5; moreover, a high molar HTS excess over cA5 is required to observe inhibition of vesicle aggregation which indicates that the interaction between annexin molecules in opposing vesicles presents a lower dissociation constant than that of HTS binding to the concave face of cA5.

Cryo-electron microscopy of aggregated lipid vesicles in the presence of wild-type annexin A4, which is structurally and evolutionary similar to annexin A5,[2,34] shows a separation compatible with two layers of membrane-bound annexin A4.[7] In contrast, annexins A1 and A2 seem to be able to induce membrane aggregation via different mechanisms in which the N-terminal domain plays an important role: membrane bridging through heterotetramers with proteins of the S100 family,[15] formation of dimers via interaction through the N-terminal domains of monomeric annexins, as suggested for annexin A4 and by us for chicken annexin A5,[16] or interaction of one molecule with two adjacent membranes simultaneously.[9,10,17]

Why does cA5 induce membrane aggregation, whereas hA5 does not? The N-terminal extension seems to be the major responsible for this different behavior as the chimera with the protein core of hA5 and the N-terminus of cA5 recovers the ability to aggregate membranes. In addition, deletion of eight amino acids from the N-terminus of cA5 strongly impairs its membrane bridging ability. One of the main differences between the N-terminus of both annexins is the higher negative charge in hA5 due to the substitution of Ala^{11} and Ala^{17} in cA5 by Asp^{11} and Glu^{17} accompanied by the replacement of Lys^3 by Gln^3

(see Fig. 10). Comparison with the N-terminus of mammalian annexin A4, which induces vesicle aggregation,[7] reveals the absence of negatively charged residues and the presence of alanines in positions equivalent to those in cA5. An increase in the negative charge in the N-terminus of bovine annexin A4 (bA4) due to phosphorylation of Thr[7] (or simulated by point mutation Thr[7] to Asp) has been reported to induce the release of the N-terminus from the protein core and impair the ability of this annexin to promote membrane aggregation.[7] A similar observation has been reported for annexin A2, where the replacement of Ser[21] or Ser[25] in the N-terminal extension by glutamic acid blocks the Ca^{2+}-dependent vesicle aggregation ability of annexin A2 by impairment of protein–protein contacts through the concave face of the annexin A2 monomers.[15] Thus, the lack of acidic residues (Asp[11] and Glu[17]) and the presence of Lys[3] and Arg[6] in cA5 N-terminal extension may be, at least partially, responsible for the membrane-aggregation ability detected in this protein and not present in the human ortholog. In fact, in dnt-cA5, where these two basic residues are not present, the ability to aggregate vesicles is significantly reduced. Additional regions of the protein may be involved in the lack of ability of hA5 to induce aggregation, as dnt-cA5 is still able to induce aggregation at high concentration and the chimera cNt-hA5 shows lower aggregation ability than the wild type chicken annexin. cA5-induced vesicle aggregation is probably dependent on the interaction between cA5 molecules through their concave faces. This region includes the N-terminal extension, the loop between domains II and III, and the C-helices from each domain of the annexin core. Interestingly, helix C from domain II shows significant charge differences between cA5 and hA5, with several acidic residues in hA5 not present in cA5 (hA5: Glu[120], Glu[130], Glu[131]; cA5: Ala[120], Met[130], Gln[131]), and Gly[166] replacing Arg[166] in cA5 (Fig. 10). In bA4, that induces vesicle aggregation,[7] residues equivalent to 130–132 in hA5 do not present negative charge (Gln[129], Leu[130], and Gln[131]). These additional negatively charged residues in the hA5 could further impair the interaction between the concave faces of hA5 due to electrostatic repulsions. The ability of hA5 to induce Ca^{2+}-dependent aggregation of PS-vesicles at mild acidic pH (in which acid lateral chains from aspartic or glutamic acid residues do not present negative charge)[36] strongly supports this model.

It is quite surprising that the two annexin A5 orthologs in human and chicken, which present a 78.1 identity and 86.9% similarity in their sequence, show a completely different behavior regarding such an important function as membrane aggregation. It has been previously reported that chicken annexin A5 resembles mammalian annexin A4 in some of its immunological and physicochemical properties, such as its apparent molecular mass and isoelectric point

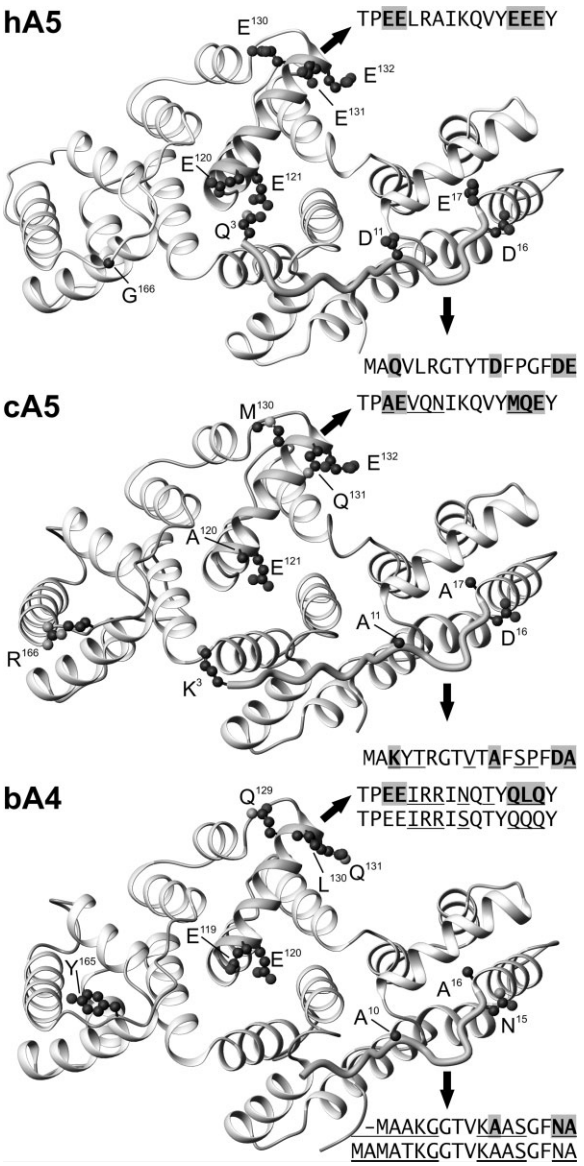

Figure 10. Three-dimensional structure of human and chicken annexin A5 and bovine annexin A4. X-Ray crystallography co-ordinates were obtained from the Protein Data Bank (hA5: 1ANX, residues 3–319; cA5: 1ALA, residues 3–320; bA4: 1ANN, residues 5–319). Molecules are viewed from the concave face and the lateral chains from the most significant residue changes between hA5 and cA5 are shown in a ball-and-stick style (Asp[16] and Glu[132] are also shown). Sequences corresponding to the N-terminal extensions and to helices IIC are shown; differences with hA5 are underlined and residues represented in a ball-and-stick style are gray-shaded. The sequences corresponding to the N-terminus and helix IIC of human annexin A4 are aligned with those from bA4. Residue numbers are assigned according to cDNA translation and thus, N-terminal methionine is Met[1] even though it is not present in the wild-type proteins. The figure was prepared using the MOLMOL program.[35]

(5.6 and 5.7 in cA5 and human annexin A4, respectively, versus 4.7 in hA5).[37] In fact, cA5 was initially misidentified as the chicken ortholog of annexin A4.[38]

In addition, annexin A4 as well as A3 and A9 genes are absent in birds (build 2.1 of the chicken genome assembly; Washington University School of Medicine in St. Louis). cA5 presents a high sequence similarity with annexins A4 and A3 (57.3% identity and 68.5% similarity with hA4, and 49.5% identity and 63.5% similarity with hA3). Thus, one could speculate that chicken annexin A5 may have evolved to gain functions that these annexins exert in other vertebrates. Calcium-dependent membrane aggregation ability may be one of this evolutionary gained functions, as this property is not present in the most ancient member of vertebrate annexins, annexin A13.[12,39]

Methods

Construction of chimeric cNt-hA5 expression vector

The cDNA from the N-terminus of chicken annexin A5 was fused to that from the core of human annexin A5 using three PCR reactions (Taq Advantage2 kit; Clontech, Mountain View, CA) according to the splicing by overlap extension technique[40] illustrated in Figure 1(A). Constructs pACII.E[20,21] and pHA5.E[22] were used as initial cA5 and hA5 cDNA templates, respectively. The final amplified fragment was first cloned into pCR2.1 (TA cloning kit; Clontech) and then into the *Nco*I/*Hin*d III sites of the pTrc99A expression vector (Pharmacia; Buckinghamshire, UK). Constructs were sequenced in both directions to verify the absence of artifacts.

Protein expression and purification

Recombinant plasmids pACII.E (cA5), pdntACII.E (dnt-cA5), pHA5.E (hA5), and pcNt-hA5.E (cNt-hA5) were transformed into JA221 *E. coli* strain. Protein production and purification was essentially performed as previously described[12,21] using the ability of the four recombinant proteins to reversibly interact with PS-enriched liposomes and a final chromatographic step in DEAE-cellulose. Pure protein preparations were dialyzed against 20 m*M* Hepes, pH 7.4, 0.1*M* NaCl, filtered through 0.22 μm membranes, and stored at 4°C until use. Protein concentration was determined by amino acid analysis (Beckman 6300 analyzer) or by UV-spectroscopy using molar extinction coefficients at 280 nm of 22,155, 20,720, 21,842, and 21,829 M^{-1} cm^{-1} for cA5, dnt-cA5, hA5, and cNt-hA5, respectively. Purity of the protein preparations was checked by SDS-PAGE followed by Coomassie blue or silver nitrate staining combined with Western blot analysis using polyclonal antibodies directed against human or chicken annexin A5 obtained in our laboratory.[41,42]

Circular dichroism measurements

CD-spectra were registered in a Jasco J-715 spectropolarimeter (Neslab RTE-111 thermostat) at 20°C in 20 m*M* Hepes, pH 7.4, containing 0.1*M* NaCl, between 190 and 260 nm in 0.05 cm-pathlength thermostatized cuvettes and using protein preparations around 0.3 mg/mL. All spectra were averaged at least over six scans and were corrected by subtracting buffer contribution from parallel spectra in the absence of protein; units are expressed as mean residue weighed molar ellipticities ($[\theta]_{MRW}$). Melting curves were determined monitoring ellipticity changes at 208 nm between 20 and 80°C and increasing temperature at 60°C/h[11,12]. Melting temperatures (T_m) were calculated from the maximum of the first derivative of the unfolding curves.

Binding to phospholipids and vesicle aggregation assays

Unilamellar vesicles were prepared using bovine brain PS (Avanti Polar Lipids, Alabaster, AL) or an equimolecular mixture PG:PC (Avanti Polar Lipids and Sigma, Alcobendas, Spain, respectively; PC from egg yolk and PG derived from egg yolk PC) by hydration of a thin dried-lipid film in 20 m*M* Hepes, pH 7.4, 0.1*M* NaCl, followed by extrusion through polycarbonate filters of either 100 or 400 nm pore diameter (Lipex Biomembranes, Vancouver, Canada). Small unilamellar vesicles (50 nm) were prepared from freshly obtained 400 nm vesicles by further extrusion through polycarbonate filters with the corresponding pore diameter.

Annexin interaction with 400 nm vesicles was carried out at a 600:1 lipid/protein molar ratio with variable calcium concentrations at 20°C for 15 min essentially as previously described.[11,12] The final mixture (300 μL) was ultracentrifuged at 134,000*g* and 4°C for 1 h (Airfuge Beckman). After separation of supernatant and pellet, equivalent aliquots were analyzed by SDS-PAGE and proteins were detected by Coomassie blue staining; gels were scanned and densitometred on a photodocumentation system from UVItec (Cambridge, U.K.) and using the UVIBand V.97 software. The percentage of bound annexin was determined from at least three independent experiments in which the supernatants and pellets were analyzed in the same gels.

Vesicle aggregation studies were performed recording absorption at 360 nm immediately after the addition of calcium to a mixture of PS unilamellar vesicles (100 nm; 0.1 mg/mL) and the corresponding annexin at 20°C or 42°C. Calcium was added from a $CaCl_2$ stock solution and absorption was registered in a thermostatically controlled cuvette for at least 15 min.[11,12] The stability of PS-vesicles in the presence of calcium concentrations up to 500 μ*M* was confirmed by the lack of self-aggregation.

Inhibition of cA5 induced vesicle aggregation by HTS (Iduron, Manchester, UK) was carried out in a slightly different manner. First, a 10 min incubation of cA5 with HTS was carried out at 20°C in the presence of 5 m*M* $CaCl_2$ at different molar ratios; afterwards,

the reaction was triggered by addition of 100 nm unilamellar PG:PC vesicles (which do not self-aggregate in the presence of 5 m*M* $CaCl_2$ as occurs with PS vesicles) from a concentrated stock (2 mg/mL) to a final concentration of 0.1 mg/mL (around 130 μ*M*). As before, aggregation was monitored at 20°C recording absorption at 360 nm immediately after addition of the vesicles.

Fluorescence emission spectroscopy

Fluorescence emission spectra were recorded between 300 and 420 nm in an SLM Aminco 8000C spectrofluorimeter at 20°C, with excitation wavelength of 295 nm and using a 0.4-cm excitation pathlength and 1.0-cm emission pathlength cuvette. Scattering was minimized by crossed Glan-Thompson polarizers. The stability of the 50 nm unilamellar PS-vesicles was verified by monitorization of the Rayleigh scattering at 90° (obtained from the maximum at 295 nm of spectra recorded at this excitation wavelength) in the absence of protein and in the presence of 200 μ*M* $CaCl_2$. Annexin binding curves to PS-vesicles were obtained plotting the fluorescence intensity ratio at wavelengths corresponding to the emission maxima from completely bound or free annexin at increasing lipid to protein molar ratios in the presence of 200 μ*M* $CaCl_2$.[11,12] The binding results have been analyzed by considering the following equilibrium:

$$P + nL \leftrightarrows PL_n$$

where P is the protein, L is the free lipid sites, and n is the number of phospholipid molecules involved at each binding site. Thus, an apparent dissociation constant (K_d) can be defined as a function of the concentration of bound ($[P]_b$) and free ($[P]_f$) protein, total PS ($[L]_t$), and n, and the following equation can be deduced:

$$\frac{[L]_t}{[P]_b} = \frac{K_d n}{[P]_f} + n$$

A plot of $[L]_t/[P]_b$ vs. $1/[P]_f$ allows the calculation of both apparent K_d and n.

Protein crosslinking in the presence of PS-vesicles

Annexin crosslinking in the presence of 100 nm PS-vesicles (600:1 and 100:1 lipid/protein molar ratios; 0.5–1.5 μ*M* protein) was carried out after a 15 min protein-vesicle interaction in the presence 200 μ*M* $CaCl_2$ using BS^3 (bis[sulfosuccinimidyl]suberate; Pierce, Rockford, IL) in a 125 molar excess for 30 min, and was stopped by addition of Tris, pH 7.4 (0.1*M* final concentration). After centrifugation for 1 h at 134,000*g*, the pellet was resuspended and analyzed by SDS-PAGE under reducing condition. Controls were carried out without PS-vesicles in the presence of 200 μ*M* $CaCl_2$ and with liposomes in the absence of calcium (1 m*M* EGTA); in these controls, no annexin was found in the pellets and the gels show crosslinked annexin in the supernatants.

Conclusion

In conclusion, we demonstrate for the first time that chicken annexin A5 is able to induce vesicle aggregation, whereas mammalian annexin A5 cannot, even though these molecules present only few differences in their amino acid sequence. Aggregation seems to involve protein to protein interactions between the concave surfaces of annexin molecules in opposing membranes. Electrostatic repulsions, mainly involving negatively charged residues in the N-terminal domain and to a lower extent in helix IIC, seem to be responsible for the inability of hA5 to induce vesicle aggregation. This property may allow cA5 to participate in additional physiological processes such as membrane trafficking.

References

1. Gerke V, Moss SE (2002) Annexins: from structure to function. Physiol Rev 82:331–371.
2. Moss SE, Morgan RO (2004) The annexins. Genome Biol 5:2.19.1–2.19.8.
3. Gerke V, Creutz CE, Moss SE (2005) Annexins: linking Ca2+ signalling to membrane dynamics. Nat Rev Mol Cell Biol 6:449–461.
4. Turnay J, Lecona E, Guzmán-Aránguez A, Pérez-Ramos P, Fernández-Lizarbe S, Olmo N, Lizarbe MA (2003b) Annexins: structural characteristics of the N-terminus and influence and influence on the overall structure of the protein. Recent Res Dev Biochem 4:79–95.
5. Turnay J, Guzmán-Aránguez A, Lecona E, Pérez-Ramos P, Fernández-Lizarbe S, Olmo N, Lizarbe MA (2003a) Influence of the N-terminal domain of annexins in their functional properties. Recent Res Dev Biochem 4:53–78.
6. Blackwood RA, Ernst JD (1990) Characterization of Ca2(+)-dependent phospholipid binding, vesicle aggregation and membrane fusion by annexins. Biochem J 266: 195–200.
7. Kaetzel MA, Mo YD, Mealy TR, Campos B, Bergsma-Schutter W, Brisson A, Dedman JR, Seaton BA (2001) Phosphorylation mutants elucidate the mechanism of annexin IV-mediated membrane aggregation. Biochemistry 40:4192–4199.
8. Naidu DG, Raha A, Chen XL, Spitzer AR, Chander A (2005) Partial truncation of the NH2-terminus affects physical characteristics and membrane binding, aggregation, and fusion properties of annexin A7. Biochim Biophys Acta 1734:152–168.
9. Hu NJ, Bradshaw J, Lauter H, Buckingham J, Solito E, Hofmann A (2008) Membrane-induced folding and structure of membrane-bound annexin A1 N-terminal peptides: implications for annexin-induced membrane aggregation. Biophys J 94:1773–1781.
10. Zibouche M, Vincent M, Illien F, Gallay J, Ayala-Sanmartin J (2008) The N-terminal domain of annexin 2 serves as a secondary binding site during membrane bridging. J Biol Chem 283:22121–22127.
11. Lecona E, Turnay J, Olmo N, Guzmán-Aránguez A, Morgan RO, Fernández MP, Lizarbe MA (2003) Structural

and functional characterization of recombinant mouse annexin A11: influence of calcium binding. Biochem J 373(Part 2):437–449.
12. Turnay J, Lecona E, Fernández-Lizarbe S, Guzmán-Aránguez A, Fernández MP, Olmo N, Lizarbe MA (2005). Structure-function relationship in annexin A13, the founder member of the vertebrate family of annexins. Biochem J 389(Part 3):899–911.
13. Rothhut B (1997) Participation of annexins in protein phosphorylation. Cell Mol Life Sci 53:522–526.
14. Bitto E, Cho W (1999) tructural determinant of the vesicle aggregation activity of annexin I. Biochemistry 38: 14094–14100.
15. Ayala-Sanmartin J, Vincent M, Sopkova J, Gallay J (2000) Modulation by Ca(2+) and by membrane binding of the dynamics of domain III of annexin 2 (p36) and the annexin 2(p11) complex (p90): implications for their biochemical properties. Biochemistry 39:15179– 15189.
16. Ayala-Sanmartin J, Zibouche M, Illien F, Vincent M, Gallay J (2008) Insight into the location and dynamics of the annexin A2 N-terminal domain during Ca(2+)-induced membrane bridging. Biochim Biophys Acta 1778: 472–482.
17. Rosengarth A, Luecke H (2003) A calcium-driven conformational switch of the N-terminal and core domains of annexin A1. J Mol Biol 326:1317–1325.
18. Ernst JD, Hoye E, Blackwood RA, Mok TL (1991) Identification of a domain that mediates vesicle aggregation reveals functional diversity of annexin repeats. J Biol Chem 266:6670–6673.
19. Andree HA, Willems GM, Hauptmann R, Maurer-Fogy I, Stuart MC, Hermens WT, Frederik PM, Reutelingsperger CP (1993) Aggregation of phospholipid vesicles by a chimeric protein with the N-terminus of annexin I and the core of annexin V. Biochemistry 32:4634–4640.
20. Turnay J, Pfannmüller E, Lizarbe MA, Bertling WM, von der Mark K (1995) Collagen binding activity of recombinant and N-terminally modified annexin V(anchorin CII). J Cell Biochem 58:208–220.
21. Arboledas D, Olmo N, Lizarbe MA, Turnay J (1997) Role of the N-terminus in the structure and stability of chicken annexin V. FEBS Lett 416:217–220.
22. Turnay J, Olmo N, Gasset M, Iloro I, Arrondo JL, Lizarbe MA (2002a) Calcium-dependent conformational rearrangements and protein stability in chicken annexin A5. Biophys J 83:2280–2291.
23. Perczel A, Park K, Fasman GD (1992) Analysis of the circular dichroism spectrum of proteins using the convex constraint algorithm: a practical guide. Anal Biochem 203:83–93.
24. Hucho F, Mullner H, Sund H (1975) Investigation of the symmetry of oligomeric enzymes with bifunctional reagents. Eur J Biochem 59:79–87.
25. de los Ríos V, Mancheño JM, Martínez del Pozo A, Alfonso C, Rivas G, Oñaderra M, Gavilanes JG (1999) Sticholysin II, a cytolysin from the sea anemone *Stichodactyla helianthus*, is a monomer-tetramer associating protein. FEBS Lett 455:27–30.
26. Oling F, Santos JS, Govorukhina N, Mazeres-Dubut C, Bergsma-Schutter W, Oostergetel G, Keegstra W, Lambert O, Lewit-Bentley A, Brisson A (2000) Structure of membrane-bound annexin A5 trimers: a hybrid cryo-EM—X-ray crystallography study. J Mol Biol 304: 561–573.
27. Oling F, Bergsma-Schutter W, Brisson A (2001) Trimers, dimers of trimers, and trimers of trimers are common building blocks of annexin a5 two-dimensional crystals. J Struct Biol 133:55–63.
28. Mo Y, Campos B, Mealy TR, Commodore L, Head JF, Dedman JR, Seaton BA (2003) Interfacial basic cluster in annexin V couples phospholipid binding and trimer formation on membrane surfaces. J Biol Chem 278:2437–2443.
29. Ladokhin AS, Haigler HT (2005) Reversible transition between the surface trimer and membrane-inserted monomer of annexin 12. Biochemistry 44:3402–3409.
30. Patel DR, Isas JM, Ladokhin AS, Jao CC, Kim YE, Kirsch T, Langen R, Haigler HT (2005) The conserved core domains of annexins A1, A2, A5, and B12 can be divided into two groups with different Ca2+-dependent membrane-binding properties. Biochemistry 44:2833–2844.
31. Capila I, Hernaiz MJ, Mo YD, Mealy TR, Campos B, Dedman JR, Linhardt RJ, Seaton BA (2001) Annexin V–heparin oligosaccharide complex suggests heparan sulfate–mediated assembly on cell surfaces. Structure 9:57–64.
32. Sopkova J, Vincent M, Takahashi M, Lewit-Bentley A, Gallay J (1999) Conformational flexibility of domain III of annexin V at membrane/water interfaces. Biochemistry 38:5447–5458.
33. Sopkova-De Oliveira Santos J, Vincent M, Tabaries S, Chevalier A, Kerboeuf D, Russo-Marie F, Lewit-Bentley A, Gallay J (2001) Annexin A5 D226K structure and dynamics: identification of a molecular switch for the large-scale conformational change of domain III. FEBS Lett 493:122–128.
34. Zanotti G, Malpeli G, Gliubich F, Folli C, Stoppini M, Olivi L, Savoia A, Berni R (1998) Structure of the trigonal crystal form of bovine annexin IV. Biochem J 329(Part 1):101–106.
35. Koradi R, Billeter M, Wuthrich K (1996) MOLMOL: a program for display and analysis of macromolecular structures. J Mol Graph 14:51–55.
36. Hoekstra D, Buist-Arkema R, Klappe K, Reutelingsperger CP (1993) Interaction of annexins with membranes: the N-terminus as a governing parameter as revealed with a chimeric annexin. Biochemistry 32:14194–14202.
37. Boustead CM, Brown R, Walker JH (1993) Isolation, characterization and localization of annexin V from chicken liver. Biochem J 291(Part 2):601–608.
38. Boustead CM, Walker JH, Kennedy D, Waller DA (1991) Crystallization and preliminary X-ray studies of annexin IV(endonexin), a calcium-dependent phospholipid-binding protein. FEBS Lett 279:187–189.
39. Iglesias JM, Morgan RO, Jenkins NA, Copeland NG, Gilbert DJ, Fernandez MP (2002) Comparative genetics and evolution of annexin A13 as the founder gene of vertebrate annexins. Mol Biol Evol 19:608–618.
40. Heckman KL, Pease LR (2007) Gene splicing and mutagenesis by PCR-driven overlap extension. Nat Protoc 2: 924–932.
41. Turnay J, Olmo N, Lizarbe MA, von der Mark K (2002b) Changes in the expression of annexin A5 gene during in vitro chondrocyte differentiation: influence of cell attachment. J Cell Biochem 84:132–142.
42. Guzmán-Aránguez A, Olmo N, Turnay J, Lecona E, Pérez-Ramos P, López de Silanes I, Lizarbe MA (2005) Differentiation of human colon adenocarcinoma cells alters the expression and intracellular localization of annexins A1, A2, and A5. J Cell Biochem 94:178–193.